# 3D gravity inversion by planting anomalous densities

Leonardo Uieda, Valéria C. F. Barbosa (Observatório Nacional, Rio de Janeiro, Brazil)



## Abstract

**This paper presents a novel gravity inversion method for estimating a 3D density-contrast distribution defined on a grid of prisms. Our method consists of an iterative algorithm that does not require the solution of a large equation system. Instead, the solution grows systematically around user-specified prismatic elements called "seeds". Each seed can have a different density contrast, allowing the interpretation of multiple bodies with different density contrasts and interfering gravitational effects. The compactness of the solution around the seeds is imposed by means of a regularizing function. The solution grows by the accretion of neighboring prisms of the current solution. The prisms for the accretion are chosen by systematically searching the set of current neighboring prisms. Therefore, this approach allows that the columns of the Jacobian matrix be calculated on demand. This is a known technique from computer science called "lazy evaluation", which greatly reduces the demand of computer memory and processing time. Test on synthetic data and on real data collected over the ultramafic Cana Brava complex, central Brazil, confirmed the ability of our method in detecting sharp and compact bodies.**

## Introduction

Over the past 20 years, substantial effort has been directed toward estimating 3D density-contrast distributions using gravity data inversion. Usually the inversion methods, like that of Li and Oldenburg (1998), produce blurred images of anomalous sources. On the other hand, methods for producing sharp images have been developed by Portniaguine and Zhdanov (2002) and Silva Dias *et al.* (2009). All previously mentioned methods require the solution of large linear systems, which can be computationally challenging for large problems. Attempts to overcome this problem include: the method of René (1986) that obtains 2D sharp and compact bodies by successively incorporating cells around pre-specified cells called "seeds" with known density contrasts; and the method of Camacho *et al.* (2000) that recovers sharp 3D bodies by means of a systematic search algorithm. We present a new 3D gravity inversion that uses "seeds" around which the density anomalies grow, as in René (1986), and imposes compactness of the solution using a regularizing function like that of Silva Dias *et al.* (2009). Tests on synthetic data and on field data collected over the ultramafic Cana Brava complex, Central Brazil, confirmed the potential of the method in producing sharp images of the density anomalies.

## Forward modeling

Consider a data set composed of $N$ observations of a gravity anomaly. We assume that these observations are due to density anomalies confined in a three-dimensional region of the subsurface. Let us consider that this region is divided into a set of $M$ juxtaposed right rectangular prisms. It follows that the gravitational attraction caused by the density anomalies can be approximated by the sum of the contribution of each prism, which can be calculated using the formulas of Nagy *et al.* (2000). Assuming that each prism has a constant density contrast, it follows that the relationship between the vertical component of the gravitational attraction and the density contrast of each prism is linear and can be expressed in matrix notation as

$$\mathbf{d} = \mathbf{G}\mathbf{p}, \tag{1}$$

where $\mathbf{d}$ is the data vector containing the vertical component of the gravitational attraction caused by the prism ensemble, $\mathbf{p}$ is the parameter vector containing the density contrast of each prism, and $\mathbf{G}$ is the Jacobian matrix of the functional relation between $\mathbf{d}$ and $\mathbf{p}$.

## Inverse problem

The inverse problem of estimating $\mathbf{p}$ is an ill-posed problem and thus requires additional constraints to be solved. The constraints used in our method impose that the solution be compact and concentrated around "seeds", which are user-specified prisms with known density contrasts. These conditions can be imposed by means of a regularizing function in a similar manner to Silva Dias *et al.* (2009). Following this approach, we formulate the inverse problem as minimizing the goal function

$$\Gamma(\mathbf{p}) = \phi(\mathbf{p}) + \mu\theta(\mathbf{p}), \tag{2}$$

where $\mu$ is a regularizing parameter. Function $\phi(\mathbf{p})$ is a measure of the data misfit, i.e., the $\ell_2$ norm of the residuals

$$\phi(\mathbf{p}) = ||\mathbf{d}^o - \mathbf{d}||_2 = \sum_{i=1}^{N}(d_i^o - d_i)^2, \tag{3}$$

where $\mathbf{d}^o$ is a vector containing the measured data and $\mathbf{d}$ is given by equation 1. Function $\theta(\mathbf{p})$ is a regularizing function that enforces the compactness of the solution around the seeds and is similar to that of Silva Dias *et al.* (2009)

$$\theta(\mathbf{p}) = \sum_{i=1}^{M}\frac{p_i}{p_i + \varepsilon}l_i^{\beta}, \tag{4}$$

where $p_i$ is the $i$th element of $\mathbf{p}$, $\varepsilon$ is a small and positive constant used to avoid discontinuities, $l_i$ is the distance between the $i$th prism and the seed to which it will be accreted, and $\beta$ is the power to which $l_i$ is raised and controls the compactness of the solution.

**Algorithm**

Our algorithm requires a set of $N_S$ seeds specified by the user beforehand. These seeds should be chosen according to prior information about the density anomalies, such as geologic models, well logs and previous inversions. Each seed consists of a prism of the interpretative model and thus the $s$th seed is described by a density contrast value $\rho_s$ and a position index $i_s$ in the parameter vector. The algorithm starts with an initial estimate $\mathbf{p}^0$ with all elements set to zero. Next, the seeds are included in the initial estimate by setting $p^0_{i_s} = \rho_s$. An iteration of the algorithm consists of trying to grow each of the $N_S$ seeds by performing the accretion of one of its neighboring prisms. The accretion of a prism to the $s$th seed is performed in three steps:

1. Each neighboring prism of the seed is temporarily added to the estimate, one at a time, and the goal function $\Gamma$ (equation 2) is evaluated for the current estimate including the neighbor. Each neighbor is added to the estimate with the density contrast $\rho_s$ of the $s$th seed.
2. One of the tested neighbors is chosen that both reduces the data-misfit function $\phi$ (equation 3) and provides the smallest value of the goal function $\Gamma$ (equation 2). This chosen neighbor is then added permanently to the estimate, finalizing the accretion. If none of the neighboring prisms of the $s$th seed meet these criteria then the $s$th seed doesn't grow in this iteration.
3. In the case that a neighboring prism is accreted to the $s$th seed, its neighboring prisms are appended to the seed's current neighbor list and the values of the goal and data-misfit functions are updated.

These three accretion steps are repeated for each seed. After all seeds have tried to grow a new iteration is started. This process stops when none of the seeds are able to grow, signifying that the data-misfit function (equation 3) cannot decrease any further. Figure 1 shows a 2D sketch of three stages of the algorithm: the starting configuration; the end of the first iteration; and the final solution.

One of the main advantages of our algorithm is that it does not require the solution of an equation system. Even more importantly, the full Jacobian matrix $\mathbf{G}$ is not needed at any one time since the search is limited to neighboring prisms of the current solution. This means that each column of $\mathbf{G}$ only needs to be calculated when the prism of the interpretative model to which it refers becomes a neighbor of the current solution. This technique is known in computer science as "lazy evaluation". Furthermore, once a neighboring prism is permanently added to the solution, it's corresponding column is no longer needed and can be discarded. This results in fast inversion times and low memory usage, allowing the inversion of large data sets using fine meshes without the need for supercomputers or data compression algorithms (Portniaguine and Zhdanov, 2002).

**Application to synthetic data**

Synthetic gravity data (Figure 2a) was used to test the performance and correctness of our method. The data was calculated at $z = 0$ km and a Gaussian error with standard deviation $0.5$ mGal and zero mean was added to the data to simulate measurement errors. The data was generated from the prismatic model shown in Figure 3a. This model consists of two outcropping prismatic bodies with different sizes and density contrasts of $0.3$ g.cm$^{-3}$ and $0.4$ g.cm$^{-3}$. A total of 87 seeds were used, all located at 500 m depth. The interpretative model is composed of 50,000 juxtaposed rectangular prisms and the data set totaled 1,250 measurements.

The final solution in Figure 3b clearly shows that our method is able to recover the geometry of both prismatic bodies, despite their strongly interfering gravitational effects. Figure 3c shows the location of the seeds inside the final result. The adjustment of the data predicted by the inversion to the synthetic data is shown in Figure 2b. It is noticeable that the data predicted by the inversion fits very closely to the synthetic, noise-corrupted data.

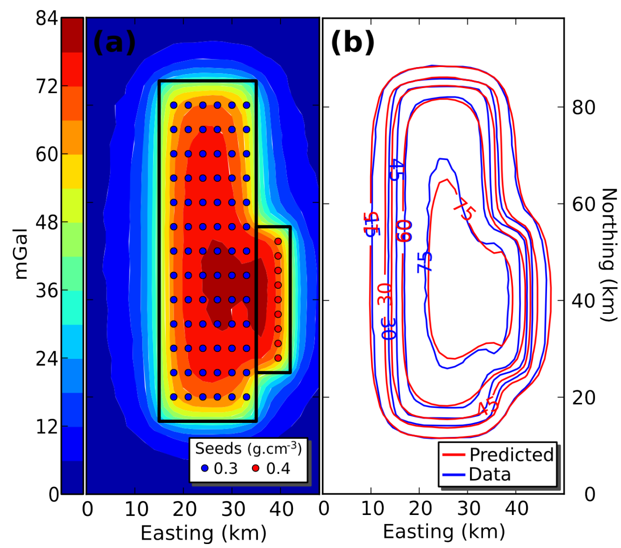


Figure 2: Test using noise-corrupted synthetic data. **a)** Synthetic data shown in a color map. Black lines denote the contour of the outcropping portion of the prismatic model. The seeds used in the inversion are represented by blue and red circles. **b)** Fit of the data predicted by the inversion (red lines) against the noise-corrupted synthetic data (blue lines).

**Application to field data**

We applied our inversion algorithm to gravity data collected over the outcropping Cana Brava layered mafic-ultramafic complex (CBC) and the Palmeirópolis volcano-sedimentary sequence (PVSS). The CBC and PVSS are located within the Tocantins Province in central Brazil, between the Amazonian and São Francisco cratons (Silva Dias *et al.*, 2009). Figure 4 shows a simplified geologic map of the CBC and PVSS and adjacent regions after Carminatti *et al.* (2003). The main host rock consists of metasedimentary sequences of the Serra da Mesa Group. Figure 5a shows the residual Bouguer anomaly map over the CBC and PVSS bodies. Carminatti *et al.* (2003) interpret the CBC as having a density contrast of $0.39$ g.cm$^{-3}$ and the PVSS of $0.27$ g.cm$^{-3}$. These values were used to generate a set of seeds at $z = 0$ km concentrated inside the outline of the outcrop. A second set of seeds located at $z = 2$ km was used for the PVSS only. The seeds are shown in Figure 5a along with the outline of the outcropping portion of the CBC and PVSS. The data set is composed of 132 measurements, the interpretative model has 432,937 prisms and the total number of seeds is 269. When performed on a computer with an Intel® Core™ 2 Duo P7350 2.0 GHz processor, the total time for the inversion was approximately 3.75 minutes.

The result of the inversion is shown in Figure 6 and is in agreement with previous interpretations by Silva Dias *et al.* (2009). The adjustment of the data predicted by the inversion to the observed gravity data is shown in Figure 5b. The fit is very close for areas where there is data (shown as + symbols) and worse for areas where data is lacking. This is expected and is most likely a product of the interpolation used for generating the contour plot.

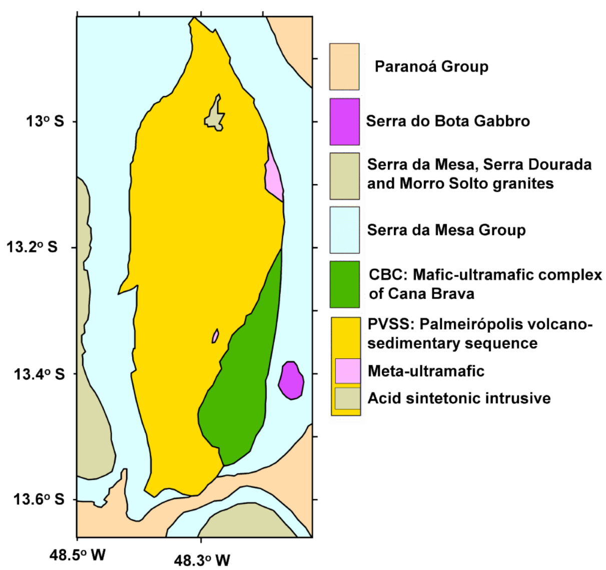


Figure 4: Simplified geologic map of the CBC and PVSS and adjacent regions, after Carminatti *et al.* (2003).

## Conclusions

We have presented a new method for linear 3D inversion of gravity data that is based on a systematic search algorithm. Prior information is incorporated into the solution by means of prismatic elements called "seeds" around which the solution is concentrated. Large data sets and fine interpretative models can be easily handled by implementing a "lazy evaluation" of the Jacobian matrix. Synthetic and field data tests show that our method is able to recover compact bodies with different density contrasts that produce strongly interfering gravitational effects. The results obtained for the Cana Brava complex are in agreement with previous interpretations.

## References

Camacho, A. G., Montesinos, F. G. and Vieira, R., 2000, Gravity inversion by means of growing bodies: Geophysics, Vol. 65, No. 1, p95-101.

Carminatti, M. G., Marangoni, Y. R., Correia, C. T., 2003, Modelagem gravimétrica do complexo de Cana Brava e

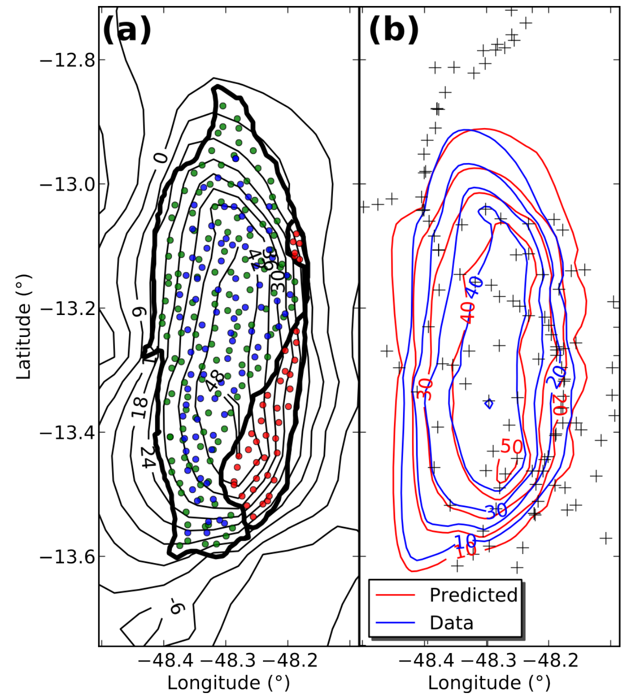


Figure 5: Gravity data of the Cana Brava complex. **a)** Residual Bouguer anomaly map, contour of the outcropping portion (black lines), and seeds used in the inversion (blue, green, and red circles). Seeds shown in blue and green have a density contrast of $0.27$ g.cm$^{-3}$ and the ones shown in red have $0.39$ g.cm$^{-3}$. Seeds in blue and red where placed at $z = 0$ km and seeds in green at $z = 2$ km. **b)** Fit of the data predicted by the inversion (red lines) against the residual Bouguer anomaly map (blue lines). Data points are shown as + symbols.

sequência de Palmeirópolis, GO: Revista Brasileira de Geociências, Vol. 33, p245-254.

Li, Y., Oldenburg, D. W., 1998, 3-D inversion of gravity data: Geophysics, Vol. 63, No .1, p109-119.

Nagy, D., Papp, G., Benedek, J., 2000, The gravitational potential and its derivatives for the prism: Journal of Geodesy, Vol. 74, p552-560.

Portniaguine, O., Zhdanov, M. S., 2002, 3-D magnetic inversion with data compression and image focusing: Geophysics, Vol. 67, No. 5, p1532-1541.

René, R. M., 1986, Gravity inversion using open, reject, and "shape-of-anomaly" fill criteria: Geophysics, Vol. 51, No. 4, p988-994.

Silva Dias, F. J. S., Barbosa, V.C.F., Silva, J.B.C, 2009, 3D gravity inversion through an adaptive-learning procedure: Geophysics, Vol. 74, No. 3, pI9-I21.

## Acknowledgments

This research is supported by the Brazilian agencies CNPq and CAPES. We thank Yára Regina Marangoni for the gravity data over the Cana Brava complex.

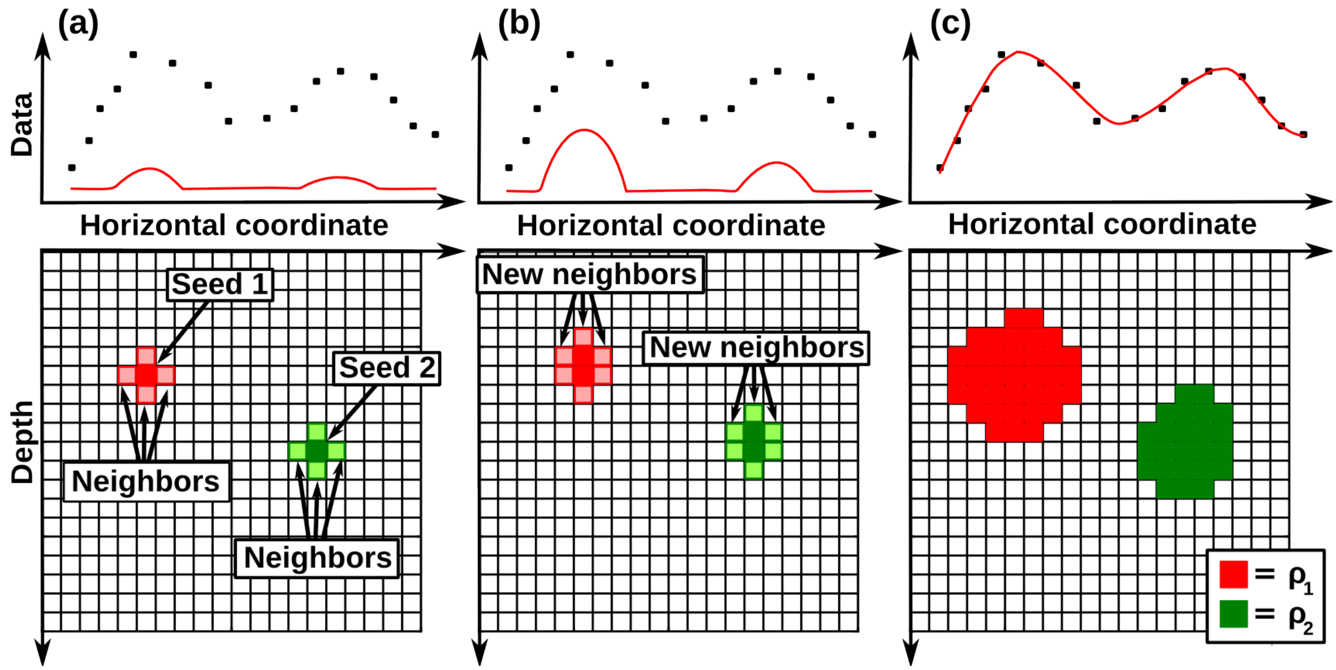


Figure 1: 2D sketch of three stages of the algorithm. **a)** Starting configuration using two seeds (dark red and dark green prisms). The neighbors of the red and green seeds are shown in light red and light green, respectively. **b)** State of the solution after the first iteration. **c)** The final result of the inversion after the algorithm stops showing compact bodies.

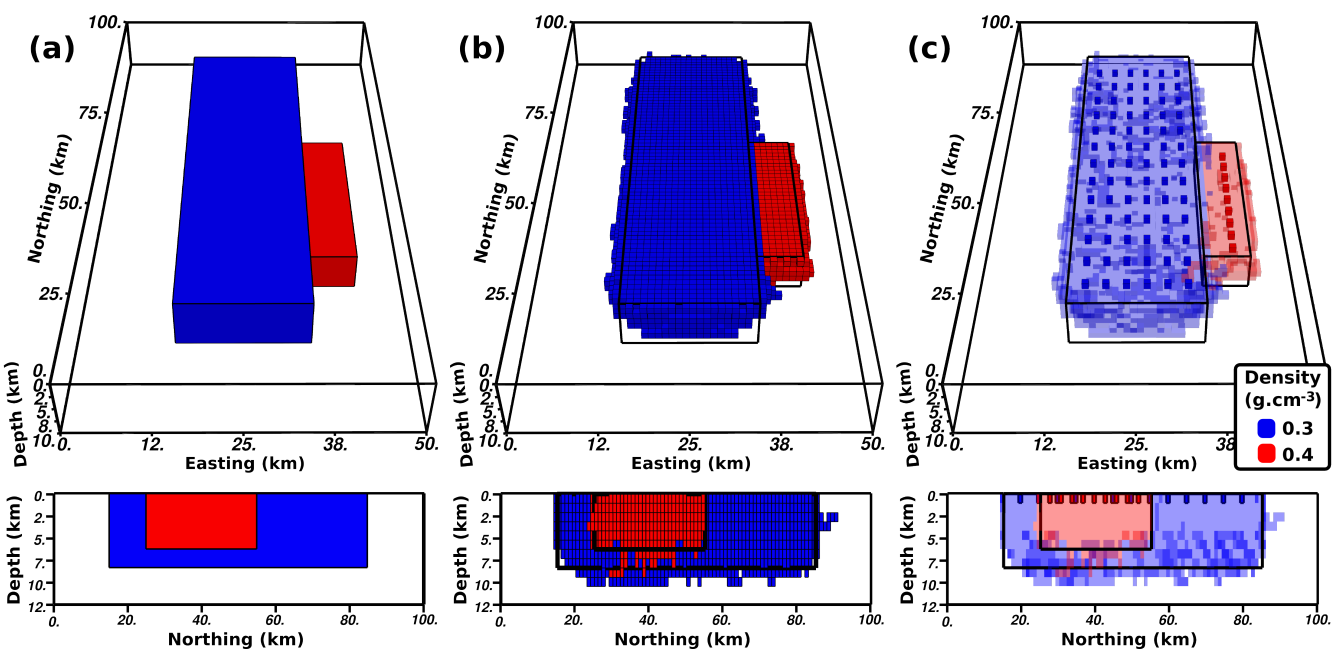


Figure 3: Results of the test using noise-corrupted synthetic data. **a)** Model composed of two juxtaposed and outcropping rectangular prisms. The prism shown in blue has a thickness of 8 km while the one in red has 6 km. **b)** Final result of the inversion. The contour of the synthetic model is shown in black lines for comparison. **c)** Seeds used in the inversion shown in dark red and dark blue. The estimated density-contrast distribution is shown with transparency for comparison.

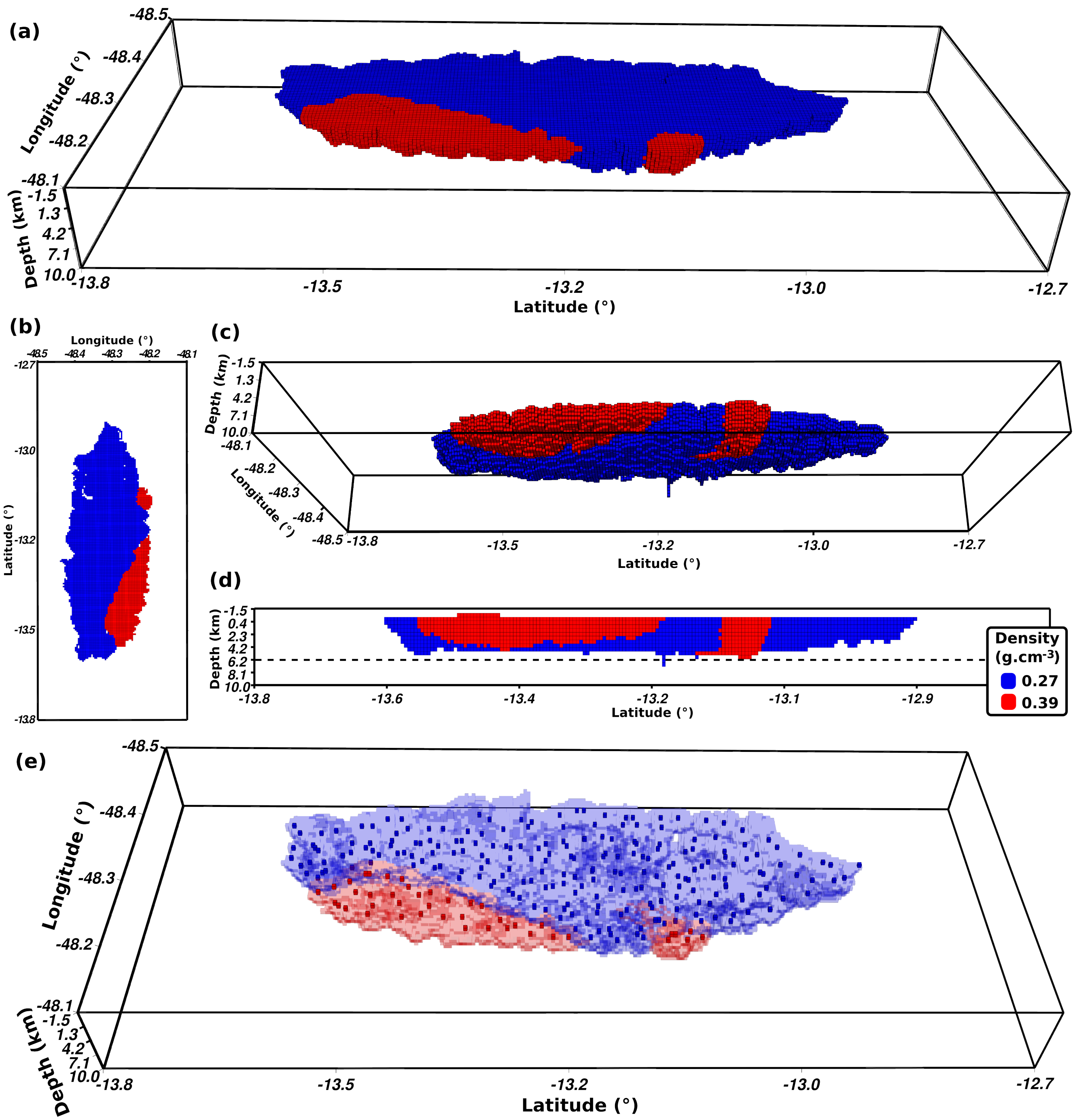


Figure 6: Result of the inversion of the Cana Brava complex gravity data. **a-d)** The estimated density-contrast distribution in different views. The maximum depth of the PVSS was approximately 6 km. **e)** Seeds used in the inversion shown in dark blue and dark red.